Measure of orbital stickiness and chaos strength

Ioannis V. Sideris*
Department of Physics, Northern Illinois University, DeKalb, Illinois 60115, USA
(Received 18 October 2005; revised manuscript received 16 February 2006; published 20 June 2006)

Patterns can be used effectively to characterize dynamical orbits as regular or chaotic. The proposed method focuses on local, epochal characterization of orbits as opposed to global characterization usually employed by most established measures. The "patterns method" provides essentially a measure of chaos strength for every extremum of a signal. For this reason, it provides information about sticky epochs of chaotic orbits, as well as time-dependent orbits. This way it can be used to give extremely detailed pictures of the phase space of a system, as well as to provide characterizations early in the evolution of orbits. Moreover, the method applies generally; all that is required is a signal, of which an orbit is merely an example.

DOI: 10.1103/PhysRevE.73.066217 PACS number(s): 05.45.−a

I. INTRODUCTION

The characterization of orbits as regular or chaotic has been a problem addressed by a number of investigators. The historically favored method is the calculation of Lyapunov exponents [1–3]. They quantify the local instability of orbits, thus they connect directly to sensitivity of initial conditions. This measure is both well justified and well established, and usually stands as the first approach to characterize the nature of orbits. In this spirit, several researchers have conceived more sophisticated methods, based on convergence of measures associated with the orbital evolution. Typical examples are the fast Lyapunov exponents [4], the helicity angles [5], the smaller alignment index method [6], as well as a new method associated with time averages related to the virial theorem [7]. These new measures are more efficient than the traditional Lyapunov exponents, since they typically converge faster.

Another class of measures relies on information derived by frequency analysis of orbits. For example, a Fourier spectrum provides a picture of the number and strength of frequencies associated with an orbit. Intuitively one expects, the more the frequencies with sizable power, the more complicated the orbit should look. Bigger complexity of the spectrum should imply bigger chaoticity [8]. Chaotic orbits are inherently more complex than regular: theoretically, they are characterized by continuous spectra, while regular orbits are characterized by discrete ones. Measures such as "complexity," which use information provided by the Fourier spectra of orbits, correlate linearly with the largest Lyapunov exponents [8,9]. In this context, more sophisticated measures have been developed [10]. Undoubtedly, they have been proven valuable in a number of different fields: celestial mechanics, galactic dynamics, and charged-particle-beam physics are only a few examples.

There are of course other measures not based on either of these two basic ideas: Kolmogorov-Sinai entropy [3] is the most typical example.

There have always been two main concerns related to chaotic measures: (a) how accurate the characterization is and (b) how fast it is, i.e., how long should one evolve an orbit to get a reliable characterization. For time-independent regimes (where energy is conserved, therefore regular orbits remain always regular, and chaotic orbits remain always chaotic during their evolution), the longer the evolution time, the more accurate the characterization. However, the shortest evolution time sufficient to claim the status of an orbit differs among measures. The traditional Lyapunov exponents may need hundreds, or even thousands, of orbital periods to converge. (To avoid confusion, the term "orbital period" is used as equivalent to one "orbital revolution," or one "dynamical time," and these terms will alternate in this paper.) The most sophisticated measures today claim to have lowered this limit to about 30 orbital periods, but this may depend significantly on both the chosen model and the specific orbit.

There are two major questions emerging: Firstly, is it possible to do better than 30 orbital periods? In some contexts, the life of systems is very short; researchers do not always have the luxury of long evolution times. Secondly, is it possible to analyze time-dependent systems? In a time-dependent regime, energy is not conserved, and orbits essentially experience a different potential at every different moment. As a result they can experience both regular and chaotic epochs, a phenomenon known as transient or intermittent chaos [11]. Dissecting orbits with the aforementioned established measures to detect short-lived chaotic or regular epochs, is either impossible by design, or at least not effective.

There is an additional problem, potentially important. The current methods provide little or no information about the sticky epochs of chaotic orbits [12–14]. It is well known that chaotic orbits, if allowed to evolve long enough, cover densely all the phase space energetically available to them. Occasionally, they get trapped for long times in confined regions of the phase space, usually located around regular islands. Physically, this entrapment is caused by the existence of dynamical obstacles in the phase space: cantori (porous tori) in two-dimensional systems, or Arnol'd webs in systems of higher dimensionality. Being trapped in these regions, they attempt to behave like regular orbits. Therefore, "stickiness" may have important physical significance in contexts such as galaxies [15], where the extent of the sticky zones may be a legitimate concern. Then, obvious questions emerge: Is it possible to contrive a method which clearly

*Electronic address: sideris@nicadd.niu.edu

identifies the sticky epochs of chaotic orbits? Most importantly, is it feasible to quantify the strength of chaos at different locations and belts of the chaotic sea? And do all the sticky regions have the same physical properties?

When a perturbation (the size of which is governed by a nonlinearity parameter k) is introduced into integrable systems, KAM theorem predicts that the invariant curves associated with irrational frequencies will deform but survive for finite values of k. When it exceeds a critical value k_c the invariant curves (two degrees of freedom) develop gaps, and transform into Cantor sets. MacKay *et al.* [16] associated the probability transition through cantori with a local flux coefficient ΔW in a Markovian model. The transport is essentially determined by the low-flux cantori but a detailed treatment needs all the cantori and the hierarchies of islands around islands to be taken into account. Meiss and Ott [17] discussed the role of this hierarchy and suggested an elegant model of transport based on Markovian trees (also Ref. [18]). The idea was that the orbit is bouncing for a long time between low-flux cantori, following essentially a random walk. The transport coefficient computed following this model was comparable to the coefficient computed numerically in other works [19,20]. In more than two dimensions, tori do not partition the energy space into independent parts, the picture is replaced by Arnol'd web, and the chaotic space is interconnected.

Summarizing, chaotic orbits evolving in time-independent potentials experience a number of different epochs during their evolution. They move through different complexity levels, from extremely sticky, when they are very close to regular islands, to wildly chaotic, when they are far from islands and well into the chaotic sea. The same is true for orbits moving in time-dependent potentials, but now since the energy is not conserved, orbits may jump from regularity to chaos and vice versa [21–23]. The main concern of most of the popular measures of chaos is distinction between chaos and regularity (one pronounced exception is Laskar's method which will be discussed shortly). This is a type of global characterization of an orbit or signal. Undoubtedly this is the most important point, but one may ask how the strength of chaos changes during the evolution of an orbit. Such information could be critical for analyzing effectively the diffusion of a chaotic orbit and the strength of the chaotic zones in time-independent potentials, as well as transitions from regularity to chaos (and vice versa) in time-dependent potentials. A measure which focuses on epochal (local) chaos strength would be a significant addition to the already existed measures.

The new measure (patterns method), presented in this paper, attempts to resolve the aforementioned issues. It treats a signal (or orbit) not as one entity but as a series of distinct epochs. In this sense, it focuses on *local*, epochal characterizations, instead of the usual approach of global characterizations. In the pictures of the phase space not only belts of stickiness are identified, but also different levels of stickiness are quantified. Pictures of the phase space can be made, including essential details, even with just ten orbital periods. Moreover, this measure should apply without any change in its logic or design to time-dependent systems. Here we focus on two-dimensional time-independent systems; work on more dimensions and time-dependent systems will be presented in future papers.

An important question is how the patterns method compares to Laskar's frequency map analysis method. This method is an excellent indicator of global dynamics and is based on an iterative scheme which determines the frequencies associated with the motion, orders of magnitude more accurately than a typical fast Fourier transform method [25]. It was first devised to analyze the stability of orbits in the solar system [10], but since then it has also been applied successfully to different contexts, such as galactic dynamics [26] and accelerator physics [27]. Accurate determination of the frequency vector of an orbit is where Laskar's method has excelled, and since the patterns method is not based on frequency analysis it would be meaningless to compare the two methods in this context.

Where the patterns method can improve on Laskar's method is on the information regarding the diffusive history of chaotic orbits. In this case Laskar's scheme computes the frequency vector ν_i of the orbit in a time-span $[t,t+T]$. This way one can follow the time evolution of frequency vector $\nu_i(t)$. It is important to notice that $\nu_i(t)$ is not an "instantaneous" frequency vector at t but instead the frequency vector of the window $[t,t+T]$. If T is not sufficiently long the frequencies cannot be determined accurately enough for a reliable study of the diffusion. A typical time T for accurate identification of frequencies ranges from 512 to 4052 iterations of a map [24,25,27].

One may ask what happens if significant transitions in the evolution of an orbit happen inside this window $[t,t+T]$. This may be the case especially within systems far from integrable, where a wildly chaotic sea is present, or within time-dependent systems where orbits can move from regular to chaotic and vice versa. Then frequency map analysis will detect a change in the frequency vector of the orbit, but it may not be able to pinpoint accurately exactly where transitions from stickiness to wild chaos happen. Also, when the whole evolution of a system is shorter than the typical value of 512 iterations the frequency map analysis may not be able to provide enough information about the diffusion of chaotic orbits without sacrificing the accuracy of the frequency vector.

A second point is that although Laskar's method can follow the diffusion of an orbit in the frequency map, it cannot (by design) provide a measure of chaos strength (or stickiness) of the orbit. It may still be possible for such information to be derived out of careful analysis of data, but it is not one of the basic features of Laskar's method. On the other hand, the patterns method was designed with characterization of chaos strength in mind. The patterns algorithm does not involve any predetermined time-span, consequently it has the advantage to pinpoint transitions in the evolution accurately even when the evolution of the system is short (how short it has to be will be carefully discussed throughout this paper). The main result (irregularity per time) for every orbit can be seen in Fig. 10 and will be discussed in Sec. V.

In Sec. II the models used for this paper are presented. In the Sec. III there is a basic demonstration about the intricate differences between regular and chaotic signals. In Sec. IV the algorithm of the method is presented. In Sec. V the nu-

merical experiments performed are elaborated. In Sec. VI there is a discussion about the new measure.

II. MODELS

Four models were used for the simulations: Hénon-Heiles potential [28], a potential of galactic type [13], the dihedral potential [29], and the standard map [13]. Exhaustive experiments were performed for the first one, and the rest were used as additional examples to test the generality of the method (pictures of the extra models are available in the supplementary material online). All four models are both well known; the main reason they were chosen was that they admit significant numbers of both regular and chaotic orbits.

The Hénon-Heiles potential is given by

$$V(x,y) = \frac{1}{2}(x^2 + y^2) + yx^2 - \frac{1}{3}y^3. \quad (1)$$

For the numerical experiments, every orbit had total energy $E=0.125$.

The potential of galactic type is given by

$$V(x,y) = \frac{1}{2}(\omega_1^2 x^2 + \omega_2^2 y^2) - \epsilon x y^2. \quad (2)$$

The choices of the parameters were $\omega_1^2=1.6$, $\omega_2^2=0.9$, $\epsilon=4.45$, and $E=0.00765$.

The dihedral potential is given by

$$V(x,y) = -(x^2 + y^2) + \frac{1}{4}(x^2 + y^2)^2 - \frac{1}{4}x^2 y^2. \quad (3)$$

The choice for the energy was $E=10.0$.

The equations of the standard map are

$$x_{i+1} = x_i + y_{i+1},$$

$$y_{i+1} = y_i + \frac{K}{2\pi}\sin(2\pi x_i) (\mathrm{mod}\ 1), \quad (4)$$

where K was chosen to be equal to 5.0.

III. SIGNALS

In this section it will be shown how a signal can be analyzed effectively to provide information about its regularity or chaos. It is both more straightforward and more pedagogical to proceed by examples.

Assume one integrates an initial condition in a potential and records, say, the variable $x(t)$ throughout the evolution (any other phase space variable could have been chosen). Essentially, the recorded data comprise a signal. By visual means only, it is often unclear whether the signal corresponds to a regular or a chaotic orbit (Fig. 1). Still, intuitively one expects the information of regularity or chaoticity to be encrypted inside the signal. Fourier analysis can decipher this information on a global level, i.e., treating the signal as one entity, but the problem can also be approached from a different point of view, to provide information on a local level. The goal is to study what the real differences between a regular and a chaotic signal are, and eventually quantify them.

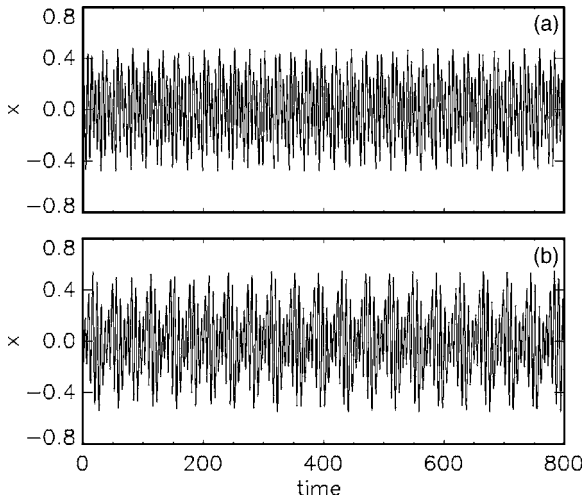

FIG. 1. The signals $x(t)$ of two orbits integrated in the Hénon-Heiles potential ($E=0.125$). One of these signals is regular and one is chaotic, but visual inspection is not sufficient to secure a reliable judgment.

The first step is to find the extrema of the signal. Intuitively, if some regularity exists it should be reflected to, and manifested through the extrema. Assume that the signal has N extrema. Now, a question can be posed: What will happen if one connects the extrema, m, $m+k$, $m+2k$, $m+3k$ and so on (in practice, the extrema that appear every k steps starting with extremum m)? In general nothing happens. However, if the signal corresponds to a regular orbit, and if an appropriate step k is chosen, smooth mono-periodic, or multiplyperiodic, curves emerge. This should be obvious from Fig. 2. For this example the step was $k=8$. Let us name this step "pattern step" for reasons that will be clarified soon. One can easily notice that there are eight smooth curves emerging (they are as many as the pattern step). These curves have obviously the same period. Hereafter this period will be called "pattern period." For this example the pattern period was about 652 time units in physical time, the equivalent of about 208 extrema.

The physical importance of pattern step and pattern period can be visualized from the plots of orbit segments in configuration space (Fig. 3). These segments show how the orbit looks between some extremum m and the extremum $m+k$ (k is always the pattern step of the signal). From these pictures one can see that the orbit "deposits" similar segments in the configuration space every k extrema. Hereafter, these "deposits" will be called "patterns." Although these patterns resemble each other, they are not the same, and they should not be. What one can observe in this picture is that, as time proceeds, the initial pattern oscillates. The successive panels can be seen as consecutive frames of a movie. This is simply a reflection of the oscillation of the smooth curve(s) emerging in the signal [Fig. 2(d)]. Eventually, after one pattern period the pattern either almost repeats (when the orbit is quasiperiodic), or exactly repeats (when the orbit is periodic).

One may try to follow the same recipe for a chaotic signal. Alas, no matter what step is chosen, no curves emerge

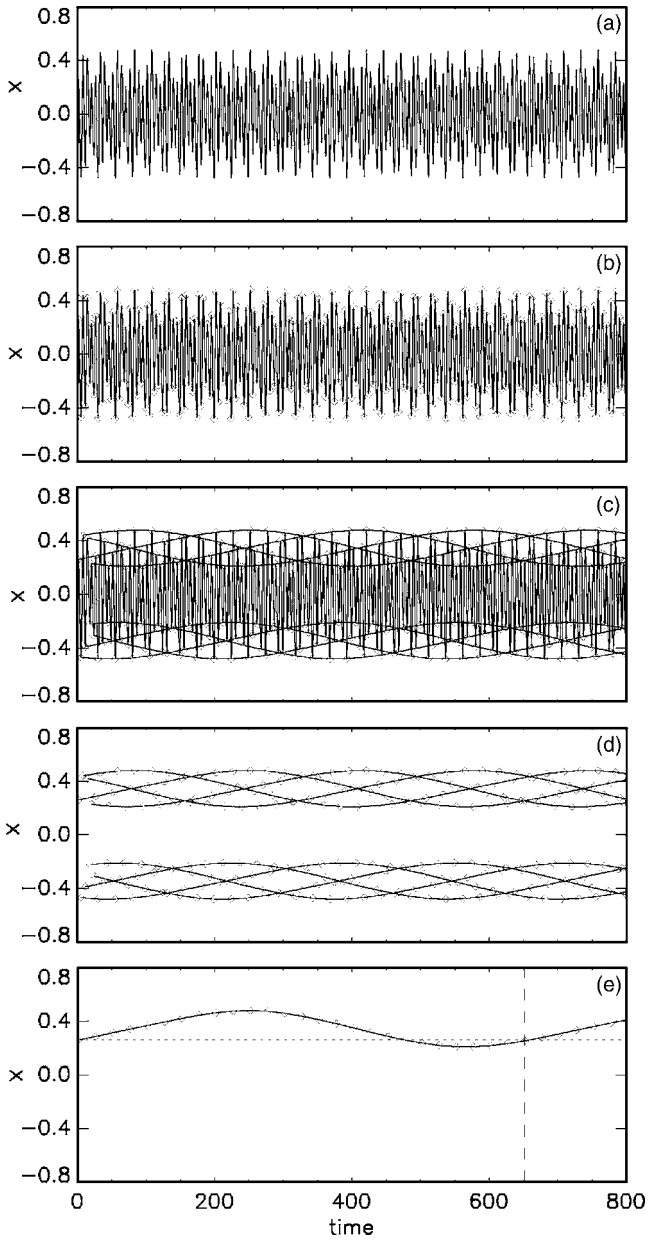

FIG. 2. (a) The signal $x(t)$ of a regular orbit evolved in the Hénon-Heiles potential ($E=0.125$). (b) The extrema of the signal interposed on the signal. (c) Smooth periodic curves emerge when the extrema of pattern step $k=8$ are connected. (d) The smooth periodic curves alone. (e) One of the eight smooth curves alone; its pattern period is $T_p=652$ time units in physical time or about 208 extrema points.

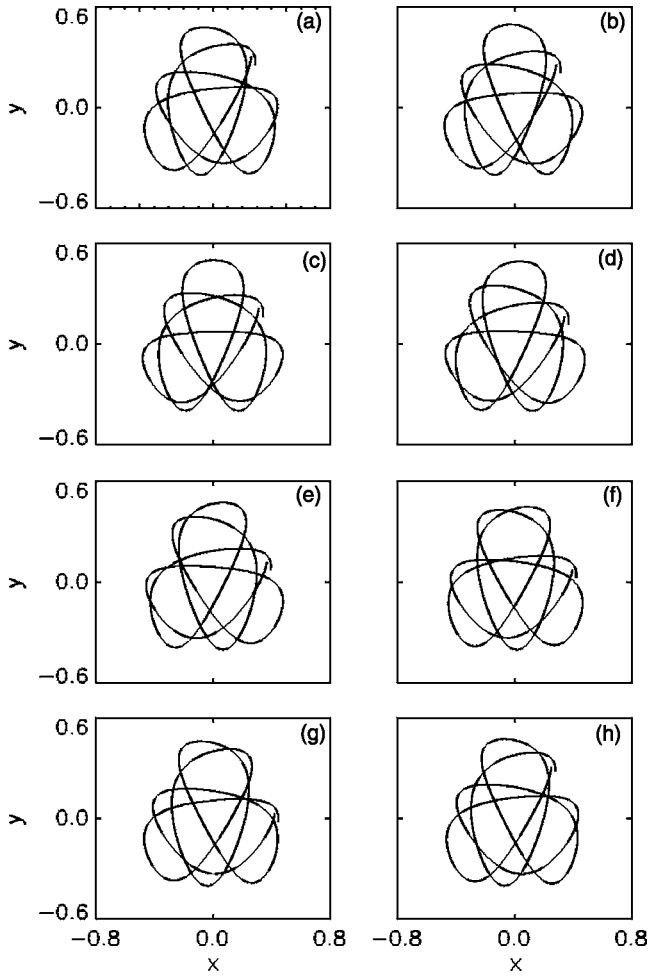

FIG. 3. Segments of the regular (quasiperiodic) orbit of Fig. 2 as it evolves in configuration space. (a) Segment between extrema 0 to 8 in signal $x(t)$ (time $t=[1.3,26.4]$). (b) Segment between extrema 8 to 16 (time $t=[26.4,51.5]$). (c) Segment between extrema 16 to 24 (time $t=[51.5,76.6]$). (d) Segment between extrema 24 to 32 (time $t=[76.6,101.7]$). (e) Segment between extrema 32 to 40 (time $t=[101.7,126.8]$). (f) Segment between extrema 40 to 48 (time $t=[126.8,151.9]$). (g) Segment between extrema 48 to 56 (time $t=[151.9,177.0]$). (h) Segment between extrema 208 to 216 (time $t=[652.0,677.1]$). This segment shows how the orbit looks after a whole pattern period. It resembles, and has to be compared with, segment (a). If the orbit was not quasiperiodic but periodic, the patterns would be exactly the same.

which are smooth in the sense manifested in regular signals. In the best case scenario, for chaotic signals one may find occasional loose regularities, curves that attempt to mimic smoothness to one extent or another (Fig. 4). Still, these curves not only do not look as smooth as the ones of regular orbits, but they are also localized in time, destined to cease to exist sooner or later. For many chaotic orbits the smoothest curves one can actually draw are simply the envelope curves of the signal (Fig. 5).

In order to have a better understanding of how the signals really behave, one can make plots of the extrema of orbits integrated for very long times (Fig. 6). Then, it becomes obvious that the extrema of periodic or quasiperiodic orbits manifest some sort of regularity. This is because of the existence of underlying smooth curves. On the other hand the extrema of chaotic orbits not only look irregular but also reveal different epochs during the evolution of the orbit: there are epochs which look completely disordered, while others possess some loose regularity. Later, it will be discussed how loose regularities associate with stickiness.

IV. ALGORITHM

How can one take advantage of the underlying patterns in a signal? Can one use these patterns to make a prediction

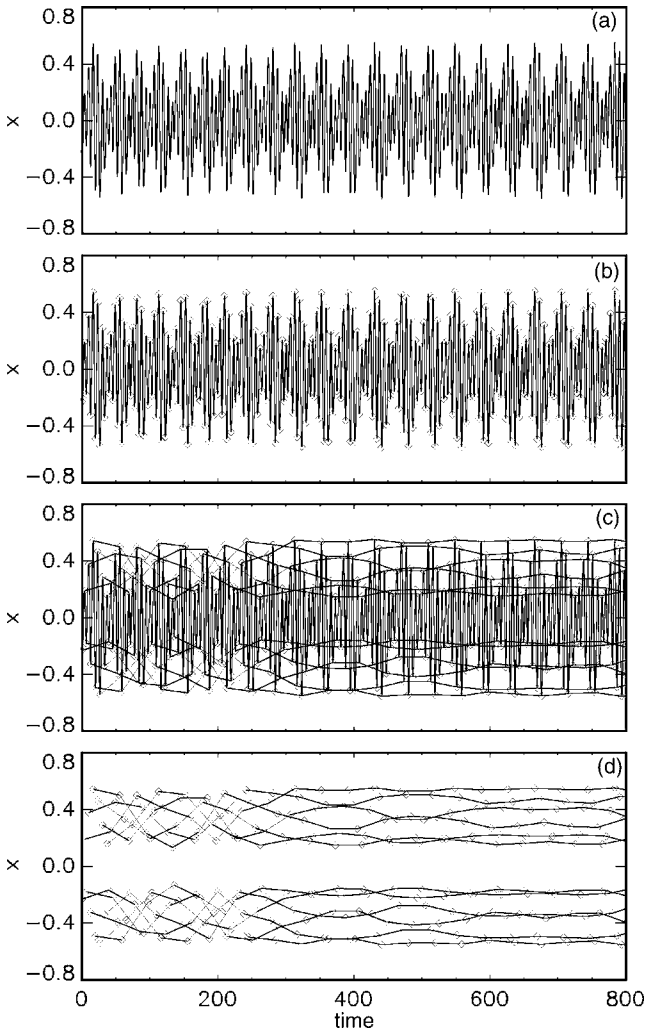

FIG. 4. (a) The signal $x(t)$ of an chaotic orbit evolved in the Hénon-Heiles potential ($E=0.125$). (b) The extrema of the signal interposed on the signal. (c) A semismooth curve emerges when the extrema points with pattern step $k=12$ are connected. (d) The twelve semismooth curves alone.

about where extrema points should appear? If one can predict to a good extent where the position of an extremum should be in a signal, then this predictability should be consistent with, or equivalent to, regularity. On the other hand, there should not be high predictability for extrema of chaotic signals.

The description of the algorithm will be done first on a local level, using an example, and then on a global, more general level. To keep the right perspective, a very important point has to be understood from the very beginning; the goal of the algorithm is to search a signal *locally*, part by part, and find the smoothest possible curve associated with every one of these parts.

For a chaotic orbit different parts can associate with different smoothest curves, therefore with different pattern steps. This is because a chaotic orbit is usually free to travel in an extensive chaotic phase space and even get sticky around different regular islands. On the other hand, for a regular orbit all the parts are described by the same pattern

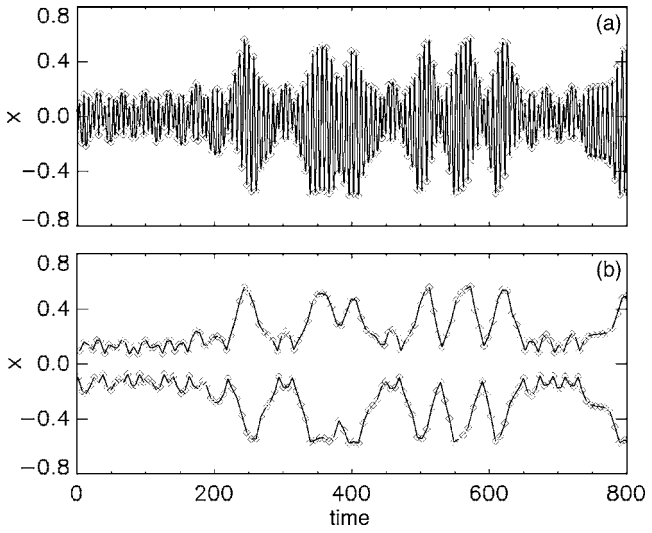

FIG. 5. (a) The signal $x(t)$ of a chaotic orbit evolved in the Hénon-Heiles potential ($E=0.125$) and the extrema of the signal interposed on the signal. (b) In practice, there is no correlation between the extrema points; the smoothest curves one can find are the ones for pattern step $k=2$, i.e., the envelope of the signal.

step; an underlying pattern simply repeats itself during evolution (Fig. 2)

Let us examine the signal in Fig. 2 carefully. This example is a regular orbit, but the analysis will be local, in one part of the signal, so it is the same as for a chaotic orbit. The pattern step for this specific signal is $k=8$. This is why eight smooth curves emerge [Fig. 2(d)]. One can assign a number i to every extremum of this signal; $i=0,1,\ldots$. The first curve comprises the extrema 0, 8, 16, 24,…, the second curve comprises the extrema 1, 9, 17, 25,…, and so on. The last (eight) curve comprises the extrema 7,15,23,31,…. Allow us to now enlarge the first part ($t=[0,80]$) of Fig. 2(d) to make the next point clear (Fig. 7).

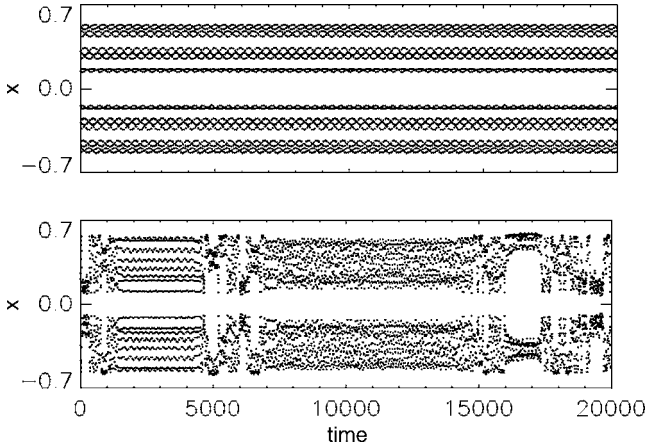

FIG. 6. Signals of two different orbits evolved in the Hénon-Heiles potential ($E=0.125$) for a very long time (20 000 time units in physical time). The first signal belongs to a regular orbit; the second one to a chaotic orbit. It is visually obvious that the chaotic orbit experiences several different epochs in the phase space. The parts that look more organized are very often associated with stickiness.

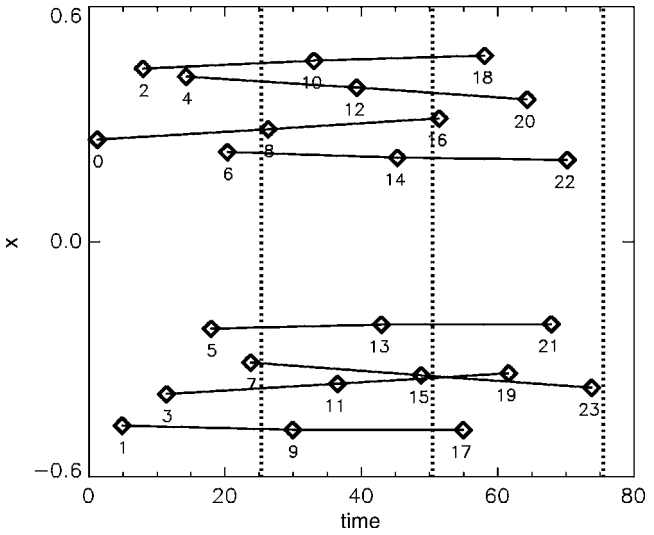

FIG. 7. The extrema and the smooth curves of the first three patterns of the signal $x(t)$ shown in Fig. 2.

Assume that one knows that, for this specific part of this specific orbit the smoothest possible curves emerge for pattern step $k=8$. (In reality we do not know from the beginning either the nature of the orbit or the pattern step, so we have to search for all possible pattern steps). One also has available the recorded values of x and t at the extrema 0 and 16, and the value of t at extremum 8. Now, to what extent is it possible to calculate the value of x at extremum 8?

The obvious next step is to use an interpolation scheme and calculate a value $x_{\text{interpolation}}$ at extremum 8, using the information from points 0 and 16. Assume one does that. Since all three points, 0, 8, and 16 belong to a smooth curve (which actually locally looks similar to a straight line) the calculated $x_{\text{interpolation}}$ value should be very close to the real value x_{real}. Then, the relative interpolation $\sigma=|(x_{\text{real}}-x_{\text{interpolation}})/x_{\text{real}}|$ can be computed.

(If we had chosen a chaotic orbit, and if we examined a part that was wildly chaotic, then the smoothest possible curve to be found would not look smooth at all. Then the relative interpolation error would be large. The same would be true for regular or sticky parts of orbits when the chosen k is not the one associated with the smoothest possible curve. So the algorithm's job is really to find the best possible k per part.)

Are the interpolation errors for all the rest of the 7 curves in Fig. 7 small? If there is regularity (locally) they should be. We repeat the process for the set of the extrema 1, 9, 17; then for the set 2, 10, 18, and so on (the last set of extrema to investigate comprises of the extrema 7, 15, and 23). The relative interpolation errors σ_i, for $i=8,9,\ldots,15$, are calculated. In practice, the extrema in 0 to 7, and 16 to 23 are used to calculate the positions of the extrema in 8 to 15.

Next, one has to find the biggest of all these interpolation errors σ_i, $i=8,9,\ldots,15$. Then this error is assigned to the extrema points 0 to 23. (In practice, this means that one can give a prediction of all the points in this pattern with accuracy smaller or equal to the biggest error). All these points were involved in the interpolation and the interpolation errors of extrema [8,15] connect inherently to the regularity associated with the extrema [0,7] and [16,23]. If the extrema in these two patterns were chaotic then the errors calculated for pattern [8,15] would be large, and vice versa.

The next step is to move to the next three patterns ([1,8], [9,16], [17,24]). Remember, there are errors already assigned to points [0,23]. One performs the same process as before, but now before the maximum error is assigned to all involved extrema points it has to be compared with the already assigned values. If the new error for some extremum is smaller than the one already assigned then the new value is kept.

Now, the process described was only for step $k=8$, However we do not really know *a priori* which pattern step will provide the smoothest curve locally. The algorithm simply has to do a search for all possible pattern steps. For every pattern step it assigns an interpolation error to every extremum. The output is a $N\times M$ matrix, where N is the number of extrema and M is the number of possible pattern steps. In addition, the whole concept can be generalized easily to interpolation orders bigger than two (for interpolation of n order, $n+1$ patterns are involved in the calculations).

Let us now talk about the general structure of the algorithm. The algorithm is comprised of the following steps. (a) Define the interpolation order n. (Start with 2 and proceed to 12 with step 2.) (b) Define the pattern step k. (Start with 1 and proceed to the biggest possible pattern step. This biggest possible pattern step depends on the order of interpolation n and the number of extrema points N.) (c) Define the patterns in the signal. How big the patterns are depends on the pattern step. (In the previous example for interpolation order $n=2$, and pattern step $k=8$, one will have $n+1=3$ patterns of 8 points each per part of the signal. The patterns will be [0,7], [8,15], and [16,23]). (d) Find the maximum interpolation errors per part as described earlier and assign them accordingly. Then move to the next part (in our example the next part will be the patterns [1,8], [9,16], and [17,24]). Find again the maximum interpolation error, compare it with the interpolation error already assigned to points [1,23] and if smaller replace the previous one. Proceed to the next part and so on. (e) Go to the next pattern step, and repeat the process. (f) Go to the next interpolation order and repeat the process.

After this process finishes 6 matrices of interpolation errors have been recorded (for interpolation orders 2, 4, 6, 8, 10, and 12). These matrices have the same number of columns (number of extrema) but different numbers of rows (number of pattern steps). As the interpolation order increases, bigger patterns are involved in every interpolation, and the maximum possible pattern step accordingly decreases.

It is interesting to mention here that if the orbit is regular a whole row (every row corresponds to a specific pattern step) will have very small interpolation errors. This means that, for some pattern step, smooth curves emerge and all the extrema are very predictable. For chaotic orbits there are isolated parts in the rows of the matrices with small interpolation errors. These parts are associated with the sticky epochs of the orbits.

The last step is to search all these matrices and find the minimum interpolation error for each extremum. This mini-

mum interpolation error will be called "irregularity" hereafter. The smaller the irregularity the more regular the particular extremum. Eventually the algorithm produces a vector of irregularities; one value of irregularity per extremum. Finally, the average and standard deviation of the vector of irregularities has to be computed as an indicator of the global behavior of the orbit.

A couple of final technical details. (a) A natural cubic spline scheme was implemented [30]. A question arises as to what the optimal order of interpolation should be. Interpolation schemes may not work very well when too many points are involved. For the experiments of this paper, interpolation order 4 or 6 usually gave the best results. Occasionally order 8 was also successful, but orders bigger than that almost never made the interpolation error smaller. Still, this algorithm used interpolations for all orders 2, 4, 6, 8, 10, and 12 just to assure best results. (b) It is better to use the absolute values of the extrema points. This way the algorithm takes advantage of symmetries in the signal, something that may be important when the integration time is limited, because it may characterize an orbit faster. (c) There are only two exceptions in the whole concept of computing interpolation errors: pattern steps 1 and 2. For pattern steps 3 or higher there are three or more curves involved in the computation of errors. In order for a pattern to look regular all these three curves should look smooth. The chance for three curves to accidentally look regular if the signal is not really regular is minimal. However, when the pattern steps are equal to 1 or 2, only one or two curves are involved. Accidentally, they may look smooth but have something to do with real regularity. Basically the statistics involved is not very good in these cases. The way one can avoid such accidents is not to allow small orders of interpolation for these particular pattern steps. For pattern step 1, orders 8 or bigger were allowed. For pattern step 2 orders 6 or bigger. This strict exception makes sure that although there are not many curves engaged, at least in the one or two used there are enough points involved.

V. EXPERIMENTS

Most of the numerical experiments were performed using the Hénon-Heiles potential. Two extra flows derived from (a) a potential of galactic type and (b) the dihedral potential, were used as additional models to demonstrate the generality of the method. The energies and parameters for all three flows were chosen to admit a significant number of both regular and chaotic orbits.

The Hénon-Heiles potential has been broadly used in the context of chaotic dynamics and astrophysics. The number of chaotic orbits it admits depends on the choice of the energy. When the energy is small there are no or few chaotic orbits. As the energy increases, the number of chaotic orbits increases and eventually dominates. The choice of the energy for the numerical experiments performed in this paper was $E=0.125$. For this energy about fifty percent of a random set of initial conditions evolve into regular orbits; the other fifty percent into chaotic.

Two sets of initial conditions were generated, each to be used for different reasons. The first one was comprised of 1000 initial conditions. These initial conditions were integrated for 1000 time units (in physical time). This is equivalent to about 150 revolutions (revolution=dynamical time =orbital period) of each orbit, or about 300 extrema points per orbit. In practice, every two extrema points are equivalent to one dynamical time. The second set was comprised of 20 000 orbits integrated for 2000 time units in physical time, or about 300 dynamical times.

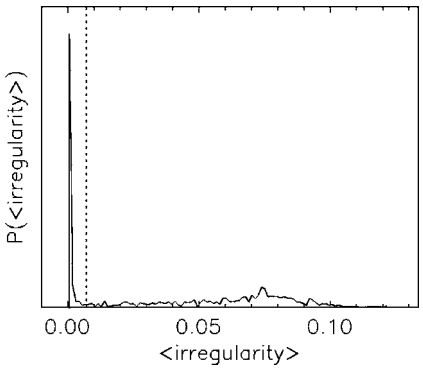

FIG. 8. The distribution of the average irregularities of 1000 orbits integrated in the Hénon-Heiles potential ($E=0.125$).

The typical process of recording the data of a Poincaré section was followed. To find the extrema of signal $x(t)$ one can simply record the data when they cross the surface $v_x=0$.

The aforementioned algorithm was applied to the orbits generated by these integrations. Irregularity was used to characterize the orbits locally at each extremum. The average irregularity was used to characterize them globally, in practice to distinguish them as regular or chaotic. In general, the difference of the average irregularity between regular and chaotic orbits is at least 1 order of magnitude, and most commonly 4 to 5 orders of magnitude; the distinction is usually clear.

There are two kinds of interesting ways to plot phase spaces using the new information. Both can be useful and are worth presenting.

A. Poincaré plots

The following demonstration refers to experiments performed on the set of 1000 orbits integrated for 1000 time units in the Hénon-Heiles potential with energy $E=0.125$. The distribution of the average irregularities of the integrated orbits was computed (Fig. 8). One can observe a sizable peak at the beginning of the x axis: regular orbits are characterized by very small average irregularities. On the other hand chaotic orbits have bigger average irregularities: their distribution disperses to a much broader area. One can distinguish where the chaotic part of the distribution starts. This distinction can establish a criterion, hereafter called "regularity threshold." Orbits with average irregularity smaller than the regularity threshold will be characterized regular, otherwise they will be characterized chaotic. For the particular set of orbits the regularity threshold is located at $\langle \text{irregularity} \rangle = 0.007$. Obviously this choice is not extremely sensitive: if it

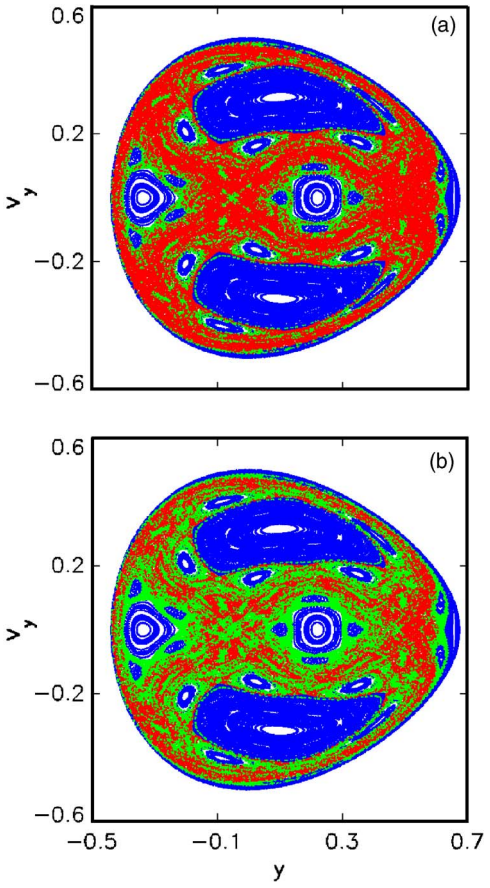

FIG. 9. (Color online) Plot of the surface section of the Hénon-Heiles potential (E=0.125). Blue (dark gray) points signify regularity, red (gray) points wildly chaotic epochs of chaotic orbits, and green (light gray) points sticky epochs of chaotic orbits. The regularity threshold was 0.007. Two different levels for the stickiness criterion are shown. (a) stickiness criterion=0.035. (b) stickiness criterion=0.065.

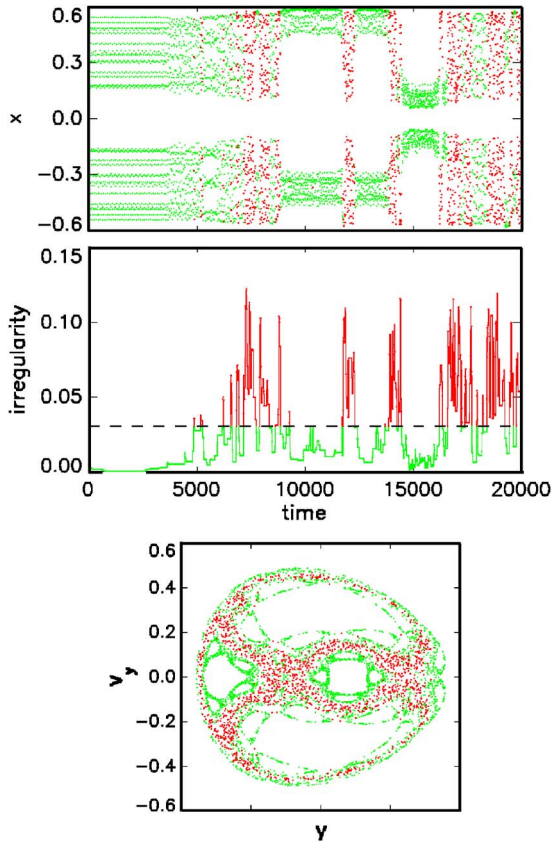

FIG. 10. (Color online). Top panel: signal of a chaotic orbit evolved in the Hénon-Heiles potential (E=0.125). The green (light gray) regions signify sticky epochs, while the red (dark gray) wildly chaotic epochs. Middle panel: the irregularity of the orbit versus time. The stickiness criterion (dashed line) has been chosen arbitrarily for demonstration reasons. Bottom panel: Poincaré section of the orbit.

was slightly bigger or smaller, only a very small number of orbits would be classified incorrectly. Such regularity versus chaos criteria are numerical necessities for other measures, too. For example when the integration time is not extremely long the largest Lyapunov exponent has not converged to zero yet, but instead to a value close to zero and one needs to establish a regularity threshold in that case too. The longer the evolution the more distinct the threshold becomes, and the same is true for the irregularity.

One can now make a plot of the phase space (Fig. 9). In this plot all points of the orbits with average irregularity less than 0.007 are considered regular and are plotted in blue. For the chaotic orbits an additional criterion has to be defined to distinguish between sticky and wildly chaotic epochs (hereafter this will be called "stickiness criterion"). However, this criterion cannot have the same nature as the regularity threshold. The reason is that there is a continuum associated with stickiness: stickiness tends to be stronger closer to the regular islands, and weakens as the distance from them increases. Sticky zones grow but they get weaker, destined to eventually intrude and disappear into the wildly chaotic region. Therefore, conceptually, a stickiness criterion should be able to show how the strength of sticky areas decreases as they grow in size, and not to distinguish sharply between sticky and wildly chaotic regions. The bigger the stickiness criterion, the broader the sticky regions are. By altering this criterion one can have pictures of how the extent of the sticky zones alters, too.

In Fig. 9 two different stickiness criteria were chosen. The sticky points were colored as green and the wildly chaotic red. As the stickiness criterion increases the size of the sticky zones increases too.

At this point it is important to show a simple example about what really happens as a chaotic orbit evolves (Fig. 10). A chaotic orbit was integrated for a very long time (20 000 time units). This orbit was chosen to be sticky in its early stages. During its evolution the orbit alternated from sticky to wildly chaotic several times. These changes are manifested in its signal, and in the calculated irregularity. When the signal looks chaotic the orbit is located inside the chaotic sea and the irregularity is bigger. For demonstration reasons only, an arbitrary stickiness criterion was chosen. In the phase space plot one can see that the method is sensible: the green points are obviously located in sticky regions, mainly around the regular islands. It is important to notice

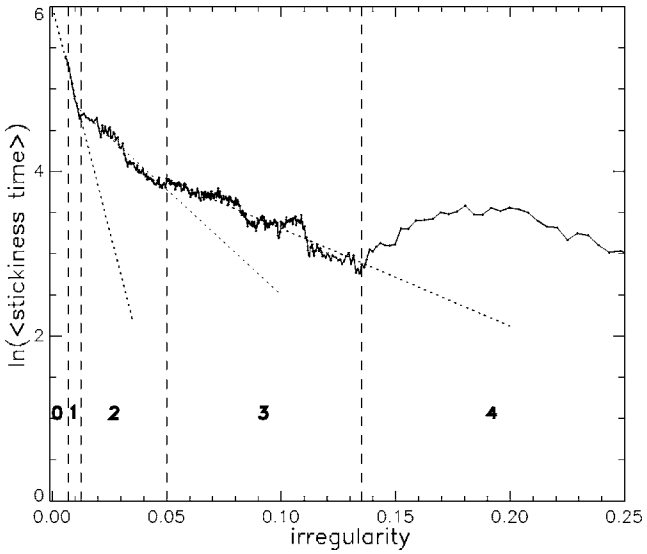

FIG. 11. Stickiness time of chaotic orbits versus irregularity in the Hénon-Heiles potential (E=0.125). Four different epochs (1 to 4) with different slopes have been identified for the chaotic orbits. (Epoch 0 pertains to regular orbits.)

that the patterns method can detect accurately transitions that happen for in very short time spans.

It is well known that the phenomenon of stickiness follows a diffusion process [31–33]. For stickiness regions around regular islands, the larger the distance from the regular island the shorter the stickiness time spent by an orbit. Irregularity should increase as the distance of an orbit from regular regions increases. Then one may try to uncover a diffusion law by performing a simple experiment. The extrema of about 10 000 chaotic orbits integrated in the Hénon-Heiles potential were analyzed to find the (stickiness) time they spent in different irregularity levels. This should be equivalent to the integration of one chaotic orbit for an extremely long time, since that orbit will cover densely all the phase space energetically available to it. In Fig. 11 one can see that the plot is divided in five different zones. Zone 0 belongs to regular orbits and is irrelevant. It extends from 0.0 to the regularity threshold 0.007. For irregularities just bigger than 0.007 the stickiness time is very large (zone 1). Stickiness is stronger close to the regular islands were the irregularity should be very small, almost comparable to the one of regular orbits. The stickiness time becomes smaller in zone 2 and even smaller in zone 3: these three zones are characterized by different slopes hinting about different properties associated with stickiness. Eventually, in zone 4 diffusion completely disappears and is replaced by a completely chaotic regime.

The four zones 1, 2, 3, and 4 were plotted in the phase space (Fig. 12) with different colors to show to what regions of the phase space they correspond. Zones 1 and 2 are plotted as green, zone 3 as red, and zone 4 as black. The existence of different zones provides quantitative information about how the chaotic sea is actually divided into areas of different properties. This information could potentially be used to establish a rigid criterion for the boundaries of important parts of the chaotic regions.

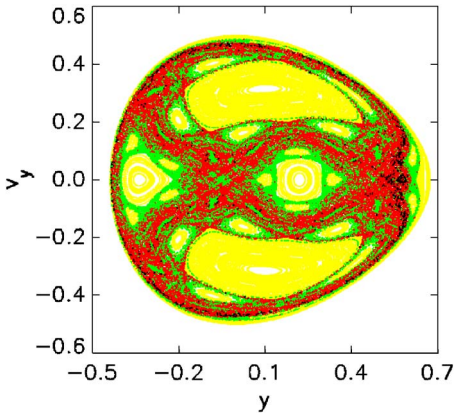

FIG. 12. (Color online). Phase space based on the diffusion information in the Hénon-Heiles potential (E=0.125). Yellow (very light gray) corresponds to Zone 0, green (light gray) signifies Zones 1 and 2, red (dark gray) signifies Zone 3 and black signifies Zone 4.

B. Contour plots

There is a second approach which can provide extremely detailed pictures of the phase space, without having to make any choice of criteria or threshold values. Since patterns method has the advantage of assigning one irregularity value to every extremum of a signal associated with an orbit, one can simply bin the data, and create a contour plot of the phase space. In order for the contour plot to be intricately detailed, 20 000 orbits were integrated for 2000 time units (physical time). Then the data were binned in a 256×256 grid. The result can be seen in Fig. 13.

Because the irregularities of typical regular and chaotic orbits differ by orders of magnitude, it is a good idea to use two plots to provide enough contour levels to show all the details of the physics involved in the phase space: one emphasizing the chaotic sea and one emphasizing the regular regions. In the plot of the chaotic sea the regular areas are green or gray (very low irregularity), and obviously very distinct. The chaotic regions start from very deep purple (very sticky) and they evolve to yellow, which signifies very large irregularity and wild chaos. Obviously, this graph provides a very rich information about the structure of the chaotic phase space. For example it can even detect the thin stickiness zones passing between the big islands; for smaller energies separatrices used to exist at those zones.

The plot of the regular areas clearly manifests that there are degrees of regularity. Full research on these degrees will be presented in a future paper, but for now it suffices to say that the new measure will probably be able to uncover interesting physical information related to the regular regions, too.

Similar experiments were performed for the a potential of galactic type and the dihedral potential. See Ref. [34] for the detailed structure of the phase space of the galactic potential (first supplement) and for the structure of the phase space of the dihedral potential (second supplement).

Finally, the same experiment was performed for the standard map. A word of caution is necessary here; the standard map involves moduli in its equations. This causes disconti-

nuities which, for small values of K, are manifested in the existence of broken tori at the edges of the phase space. Such discontinuities do not appear or make sense in usual flows. Exactly because of these discontinuities there are orbits for which the algorithm does not function properly. This happens because some of the smooth curves are replaced by step functions. This is a point that is worthy of future research. Still the algorithm can characterize correctly significant parts of the phase space even for small K. It can be applied almost safely for choices of K where broken tori do not exist at the edge of the phase space. The result for $K=5$ can be seen in the supplementary material. Again there is a rich structure revealed in the phase space. See Ref. [34] for the detailed structure of the phase space of the standard map (third supplement).

C. Short-time evolution

One may ask what happens when the available evolution time of a system is extremely limited. This method can identify regularity after three patterns have been formed. If the evolution time of the system is shorter than that, the algorithm will fail. The question emerging is, does a significant number of regular orbits form three patterns early in their evolution?

To answer this question one has to show how the phase space looks as the evolution time decreases. In Fig. 14 one can see the distributions of average irregularity, the phase space plots and the contours for evolution times equal to 200 (about 30 dynamical times), 100 (about 15 dynamical times), and 70 (about 10 dynamical times). The regularity versus irregularity threshold has been defined by the distribution plots. As is obvious, determining this threshold accurately becomes more and more difficult/arbitrary as the evolution time decreases. For the last series of panels (10 dynamical times) the choice is obviously highly arbitrary. However, the pictures of the contours do not involve any arbitrary choices of parameters, can be considered more objective, and succeed to show where the system is more regular and where irregularity increases.

It is clear from these plots that the algorithm works quite well for 30 dynamical times. For 15 dynamical times the picture is still clear although small regular islands cannot be identified any more. Even for 10 dynamical times the pictures still provide enough information in the sense that it clearly identifies many important regions of regularity.

VI. DISCUSSION

The strongest point of the new measure is that it can identify epochal regularity and assign a local chaos strength. This is a significant advantage over other measures, in the sense that a chaotic orbit is usually neither globally sticky, nor globally wildly chaotic; instead it can experience both behaviors throughout its evolution. The new measure can identify and distinguish between different evolutionary epochs and quantify them accordingly.

There are two limitations inherent in this method. (a) Orbits can be quantified correctly only when their integration

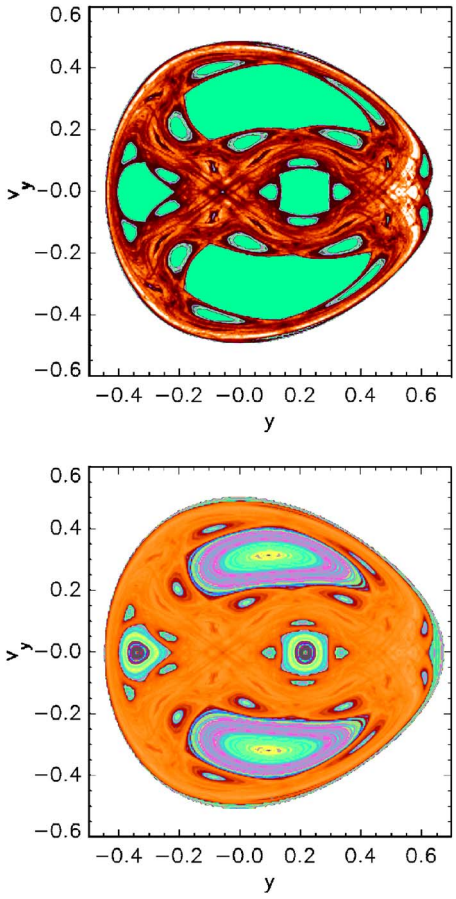

FIG. 13. (Color online). Contour plot of the phase space of Hénon-Heiles potential ($E=0.125$). In the top panel emphasis is given to the chaotic region. The regular regions are easily distinguishable as green (very light gray) or light gray. Sticky regions have bigger irregularities than regular, and appear as deep purple (very dark gray). As irregularity increases the chaotic regions become lighter purple and for very irregular regions they become yellow (in the grayscale version this can be seen as different shades of gray inside the chaotic sea; deeper gray shades correspond to bigger stickiness). In the bottom panel emphasis is given to the regular areas. Irregularity is different in different

time is at least three times their pattern step. In other words, they must have formed at least three patterns. As the integration time decreases the method fails for more and more orbits. (b) A small number of chaotic orbits start and stay extremely sticky during their evolution. These orbits mimic regular orbits quite persuasively. Fortunately their number in a typical random set of orbits is usually very small. The patterns method will probably characterize these orbits as regular.

There is no absolute remedy for the first problem. If an orbit has not been evolved long enough to form at least three patterns, the algorithm does not have enough information to quantify it correctly. It is true, though, that at least for the Hénon-Heiles case the big majority of orbits formed three patterns over a small number of dynamical times. It is worth mentioning here that the standard deviation of the irregularities of the extrema of regular orbits is very small. This is because regular orbits do not experience tremendous changes

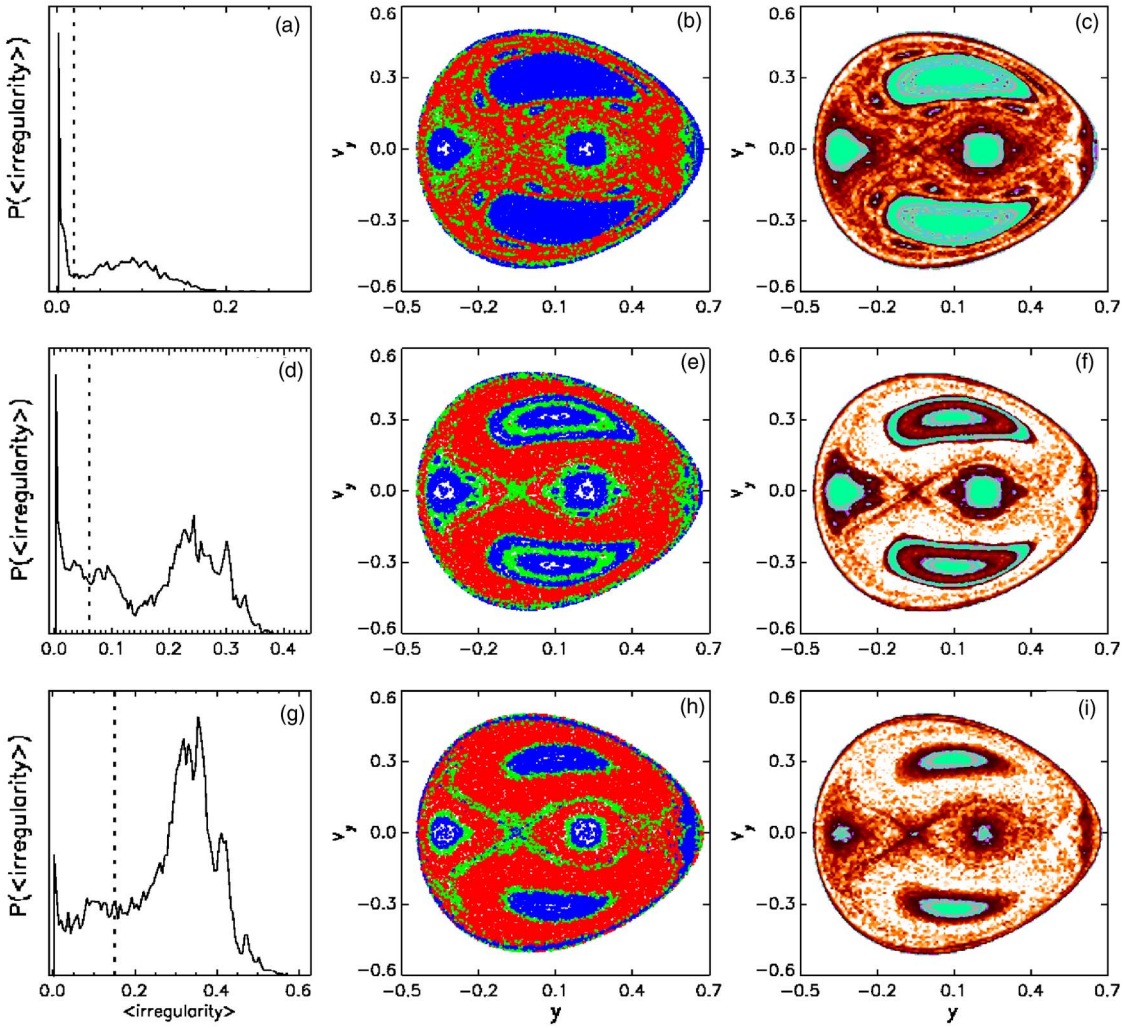

FIG. 14. (Color online). Distributions of average irregularity, Poincaré sections, and contour plots of the phase space of the Hénon-Heiles potential (E=0.125) for short evolution times. Top panels: evolution time=200 (equivalent to about 30 dynamical times). Middle panels: evolution time=100 (equivalent to about 15 dynamical times). Bottom panels: evolution time=70 (equivalent to about 10 dynamical times).

in irregularities as chaotic orbits do. This may end up being an additional criterion of regularity versus chaoticity, one that could provide some sort of characterization information even for extremely short times. Future research will carefully address this possibility.

One may ask how the average irregularity converges in time. This is shown in Fig. 15 for typical regular, and typical chaotic orbits in the Hénon-Heiles potential. In this plot one can see that the average irregularities of regular orbits converge very fast. On the other hand, it takes much longer for the average irregularities of chaotic orbits to converge. This happens because the phase space energetically available to chaotic orbits is typically bigger than the one available to regular orbits; it is not constrained by the existence of local integrals. A second important point is that the chaotic curves stay away from zero. Occasionally at some point of the evolution they may approach zero (which reflects sticky epochs), but not as close as regular orbits do. The earlier a sticky epoch happens, the closer the curve will approach zero. Eventually, chaotic orbits converge to values distinctly far from zero. It is interesting that if allowed to evolve for long enough, different chaotic orbits seem to converge slowly to similar values. This is not a surprise: the longer chaotic orbits are allowed to evolve, the denser they cover the phase space energetically available to them, unavoidably experiencing similar epochs, thus ending up converging to a similar average irregularity. In practice, they all result in having the same statistical properties.

One should not expect the average irregularity to have a linear relationship with any of the existing measures that characterize an orbit globally. The design and logic of the patterns algorithm focuses on local characterization of orbits. There is no reason that an average of these characterizations should correlate linearly with measures designed to provide global characterization. The relationship between irregularity and local instability during the evolution of a chaotic orbit is not clear.

On the other hand, one should expect this method to agree with the established measures on the distinction between regularity and chaos. The plots already presented strongly suggest that this is true. Specifically, the characterization of orbits (as regular or chaotic) computed by the new method

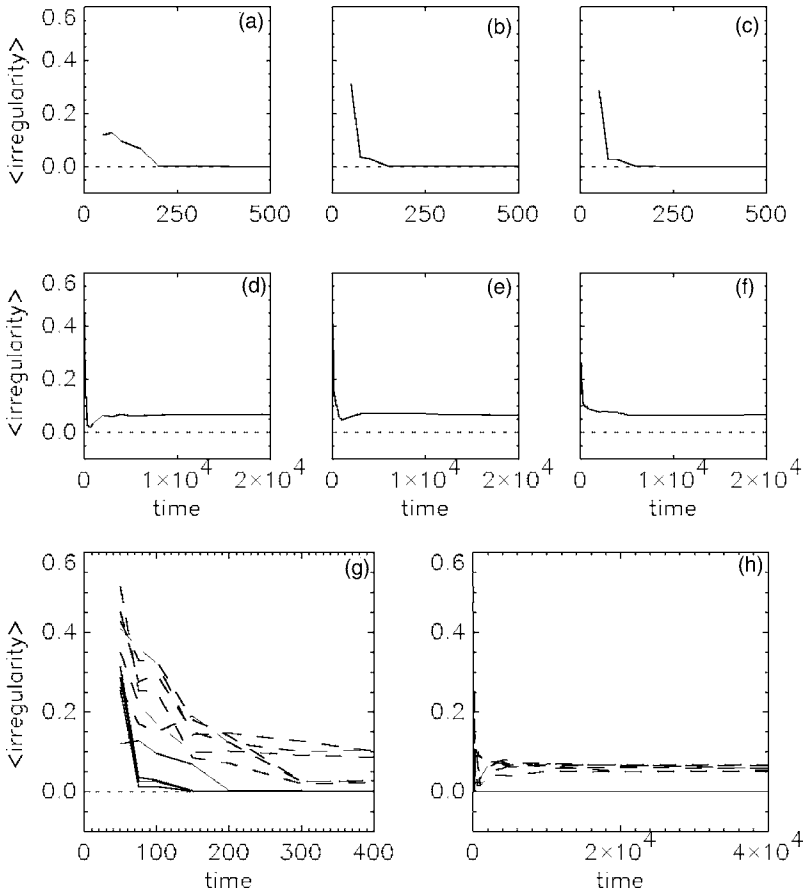

FIG. 15. (a), (b), and (c): Convergence of the average irregularity for three typical regular orbits in the Hénon-Heiles potential (E=0.125). (d), (e), and (f): Convergence of average irregularity for three typical chaotic orbits in the same potential (notice that the time scale is different from the top three panels). (g) The curves of typical chaotic orbits (dashed lines) are located higher than the curves of regular ones (solid lines). (f) Same as (g) but for longer evolution.

for the 1000 orbits, which evolved in Hénon-Heiles for about 150 dynamical times, agreed up to almost 99% with the characterization provided by the computation of their largest Lyapunov exponents. If one uses the extra information from the standard deviation of irregularity (which has to be small for regular orbits) this percentage ascends to almost 100%, failing only in extremely pathological cases. Longer evolution always increases the percentage of success.

Since the logic of this measure is based on local identification of irregularity, it can be used directly in time-dependent potentials. A whole treatment of this idea will be presented soon in a follow-up paper, but the whole theme is very important in the sense that it provides a way of identification of regularity versus chaos in time-dependent systems.

It is extremely important that this measure should be able to work equally well for orbits that have been integrated in smooth potentials, N-body systems, or in any physical system in general (with the exception of artificial systems with inherent discontinuities). This happens because it searches for regularity in signals. There are many different contexts in physics and industry where the only information about a system is data associated with the measurement of a variable, in practice a signal. Then, one can use this algorithm to analyze it. Therefore, the whole idea can potentially extend to a much wider spectrum of contexts, essentially wherever one needs to make a judgment about epochal regularities or irregularities of a signal.

It has to be mentioned that this algorithm is very effective. Although it is an $O(N^2)$ algorithm, N is the number of extrema of the signal, and therefore often small. However, there are contexts for which it may be large. Then the best idea would be to divide orbits in relatively big pieces, and then analyze these pieces.

Concerning future plans there is additional physics associated with the existence of underlying smooth curves and patterns. This physics deserves a thorough investigation, which the author plans to perform and present in a future paper. In this paper the main goal was to introduce the idea and to present an algorithmic approach of how to take advantage of it. Also, it has to be shown how the patterns method applies to systems with more that two degrees of freedom. The treatment of the one-dimensional signals of multidimensional systems should be the same as in two dimensions; still a careful analysis is necessary to demonstrate that there are no problems arising. Finally how this method applies to time-dependent systems is a question of major interest, and a future paper will carefully address it.

ACKNOWLEDGMENTS

I would like to thank Courtlandt Bohn for his support and encouragement with this project. I also want to thank both Courtlandt Bohn and Balša Terzić for interesting comments and conversations. This work was supported by Air-Force Contract No. FA9471-040C-0199.

[1] A. M. Lyapunov, Ann. Math. **17**, 1947 (1907).
[2] G. Benettin, L. Galgani, A. Giorgilli, and J.-M. Strelcyn, Meccanica **15**, 9 (1980); **15**, 21 (1980).
[3] A. J. Lichtenberg and M. A. Lieberman, *Regular and Chaotic Dynamics* (Springer-Verlag, New York, 1992).
[4] C. Froeschle, E. Lega, and R. Gonczi, Celest. Mech. Dyn. Astron. **67**, 41 (1997).
[5] G. Contopoulos and N. Voglis, Celest. Mech. Dyn. Astron. **64**, 1 (1996).
[6] C. Skokos, J. Phys. A **34**, 10029 (2001).
[7] J. E. Howard, Celest. Mech. Dyn. Astron. **92**, 219 (2006).
[8] H. E. Kandrup, B. L. Eckstein, and B. O. Bradley, Astron. Astrophys. **320**, 65 (1997).
[9] C. L. Bohn and I. V. Sideris, Phys. Rev. ST Accel. Beams **6**, 034203 (2003).
[10] J. Laskar, Icarus **88**, 266 (1990).
[11] H. E. Kandrup, I. M. Vass, and I. V. Sideris, Mon. Not. R. Astron. Soc. **341**, 927 (2003).
[12] R. B. Shirts and W. P. Reinhardt, J. Chem. Phys. **77**, 5204 (1982).
[13] G. Contopoulos, *Order and Chaos in Dynamical Astronomy* (Springer-Verlag, Berlin, 2002).
[14] G. Contopoulos, Astrophys. J. **76**, 147 (1971).
[15] E. Athanassoula, O. Bienyam, L. Martinet, and D. Pfenniger, Astron. Astrophys. **127**, 349 (1983).
[16] R. S. MacKay, J. D. Meiss, and I. C. Percival, Phys. Rev. Lett. **52**, 697 (1984).
[17] J. D. Meiss and E. Ott, Phys. Rev. Lett. **55**, 2741 (1984).
[18] J. D. Meiss, Photochem. Photobiol. **74**, 254 (1994).
[19] C. F. F. Karney, Physica D **8**, 360 (1983).
[20] B. V. Chirikov and D. L. Shepelyanksi, Physica D **13**, 394 (1984).
[21] I. V. Sideris (unpublished).
[22] C. L. Bohn and B. Terzić (unpublished).
[23] C. L. Bohn, G. T. Betzel, and I. V. Sideris, Nucl. Instrum. Methods Phys. Rev. A (to be published).
[24] J. Laskar, in Proceedings of NATO ASI Hamiltonian Systems with Three or more Degrees of Freedom, edited by C. Simo (Kluwer, Dordrecht, 1999), pp. 134–150.
[25] J. Laskar, Physica D **67**, 257 (1993).
[26] Y. Papaphilippou and J. Laskar, Astron. Astrophys. **307**, 427 (1996).
[27] H. S. Dumas and J. Laskar, Phys. Rev. Lett. **70**, 2975 (1993).
[28] M. Hénon and C. Heiles, Astrophys. J. **69**, 73 (1964).
[29] D. Armbruster, J. Guckenheimer, and S. Kim, Phys. Lett. A **140**, 416 (1989).
[30] W. H. Press, S. A. Teukolsky, W. T. Vetterling, and B. P. Flannery, *Numerical Recipes in C* (Cambridge University Press, New York, 1993).
[31] C. Efthymiopoulos, G. Contopoulos, N. Voglis, and R. Dvorak, J. Phys. A **30**, 8167 (1997).
[32] D. Bensimon and L. P. Kadanoff, Physica D **13**, 82 (1984).
[33] R. S. MacKay, J. D. Meiss, and I. C. Percival, Physica D **13**, 55 (1984).
[34] See EPAPS Document No. E-PLEEE8-73-198605 (Supplement 1) for the detailed Structure of the galactic potential, (Supplement 2) for the structure of the dihedral potential, and (Supplement 3) for the detailed structure of the phase space of the standard map. For more information on EPAPS, see http://www.aip.org/pubservs/epaps.html/.